

Magnetic percolation and giant spontaneous Hall effect in $\text{La}_{1-x}\text{Ca}_x\text{CoO}_3$ ($0.2 \leq x \leq 0.5$)

A. V. Samoilov

Department of Physics 114-36, California Institute of Technology, Pasadena, California 91125

G. Beach

*Department of Physics 114-36, California Institute of Technology, Pasadena, California 91125
and Center for Space Microelectronics Technology, Jet Propulsion Laboratory, California Institute of Technology,
Pasadena, California 91109*

C. C. Fu and N.-C. Yeh

Department of Physics 114-36, California Institute of Technology, Pasadena, California 91125

R. P. Vasquez

*Center for Space Microelectronics Technology, Jet Propulsion Laboratory, California Institute of Technology,
Pasadena, California 91109*

(Received 23 February 1998)

We report an unprecedentedly large spontaneous Hall effect in ferromagnetic $\text{La}_{1-x}\text{Ca}_x\text{CoO}_3$ ($0.2 \leq x \leq 0.5$) epitaxial films. The effect exceeds existing theoretical predictions for the value of the spontaneous Hall resistivity ρ_{xy} by several orders of magnitude. The Hall effect is the strongest for $x=0.2$, which is at a doping level nearest to the ferromagnetic percolation threshold in $\text{La}_{1-x}\text{Ca}_x\text{CoO}_3$. We suggest that the coexistence of high- and low-spin configurations in the perovskite cobaltites, together with the magnetic percolation behavior, may be responsible for the giant Hall effect. [S0163-1829(98)51822-X]

Magnetotransport in mixed-valent manganese oxides with perovskite structure¹ in heterogeneous (layered or granular) metallic systems² is a recent subject of great interest, because of the significant reduction in the electrical resistance when a magnetic field is applied. This property is referred to in the literature as the colossal and giant magnetoresistance (CMR and GMR) of perovskite manganites and of binary metallic systems, respectively. Along with the magnetoresistance, another important magnetotransport property, the Hall effect, has been studied.³⁻⁶ Generally speaking, the Hall resistivity ρ_{xy} of a magnetic metal may be expressed in terms of two contributions: $\rho_{xy} = R_0 B + R_s(\mu_0 M)$, where $R_0 = 1/(ne)$ is the Hall coefficient due to the Lorentz force on the conducting carriers of a density n and charge e , B is the magnetic induction, and R_s is the anomalous Hall coefficient associated with the magnetization M of the sample. Theory⁷ attributes the anomalous Hall effect to the asymmetric (skew) scattering of carriers relative to the plane spanned by M and the electrical current or to the side-jump mechanism.⁸ In the case of granular GMR films, Wang and Xiao have found⁶ that the surface-induced spin-orbit interaction significantly influences the anomalous Hall resistivity. On the other hand, no evidence for an anomalous Hall effect has been reported in the perovskite manganites.⁴

In this paper, we report an unprecedentedly large spontaneous Hall effect in the rare-earth perovskite cobaltites, $\text{La}_{1-x}\text{Ca}_x\text{CoO}_3$ ($0.2 \leq x \leq 0.5$). The magnitude of R_s is found to exceed existing theoretical predictions^{12,13} by several orders of magnitude. The significant doping dependence of the Hall resistivity, together with the magnetic heterogeneity⁹⁻¹¹ (see below) of these crystallographically single-phase materials, strongly suggests the importance of the magnetic per-

colation behavior, thereby lending new insights into the physical origin of the anomalous Hall effect.

In the parent compound of the mixed-valent perovskite cobaltites, LaCoO_3 , the crystal-field splitting is larger than the exchange of Hund's energy.⁹ Therefore, at low temperatures, the trivalent Co ions have a low-spin $t_{2g}^6 e_g^0$ (with spin $S=0$) configuration (Co^{III}). The substitution of divalent atoms (i.e., Sr or Ca) results in the appearance of tetravalent Co^{4+} ions which polarize the oxygen p electrons and reduce the crystal-field effect on the trivalent Co ions, hence stabilizing the high-spin $t_{2g}^4 e_g^2$ (Co^{3+}) configuration. As a result, magnetic clusters [$\text{Co}^{4+}-6\text{Co}^{3+}$] are formed near each Ca atom.⁹ With increasing doping levels, the magnetic clusters reach a magnetic percolation threshold at $x \approx 0.15$. Chemically doped holes (associated with Co^{4+}) induce ferromagnetism via the so-called double-exchange interaction.¹⁴ $\text{La}_{1-x}\text{Sr}_x\text{CoO}_3$ is found to have a metallic electrical conduction for $0.3 \leq x \leq 0.5$, with "hole-poor," lower-spin matrix interpenetrating the metallic "hole-rich," higher-spin regions.⁹ In $\text{La}_{1-x}\text{Ca}_x\text{CoO}_3$ (LCCO) the Curie temperature increases with increasing x and saturates at $T_c = 180 \text{ K} - 185 \text{ K}$ for $x > 0.3$.¹¹

The $\text{La}_{1-x}\text{Ca}_x\text{CoO}_3$ epitaxial films ($x=0.2, 0.3, 0.5$) are grown by pulsed laser deposition using stoichiometric targets of $\text{La}_{1-x}\text{Ca}_x\text{CoO}_3$ in 100 mTorr of oxygen. The temperature of the LaAlO_3 substrates is 700 °C. The growth is followed by annealing in 1 atm oxygen at 900 °C for 10 h. All samples are single-phase materials, as characterized by x-ray diffraction, and the epitaxy of the films is confirmed by x-ray rocking curves. The Hall effect is studied in thin film samples which are (2-5) mm × (2-5) mm × (100-300) nm in

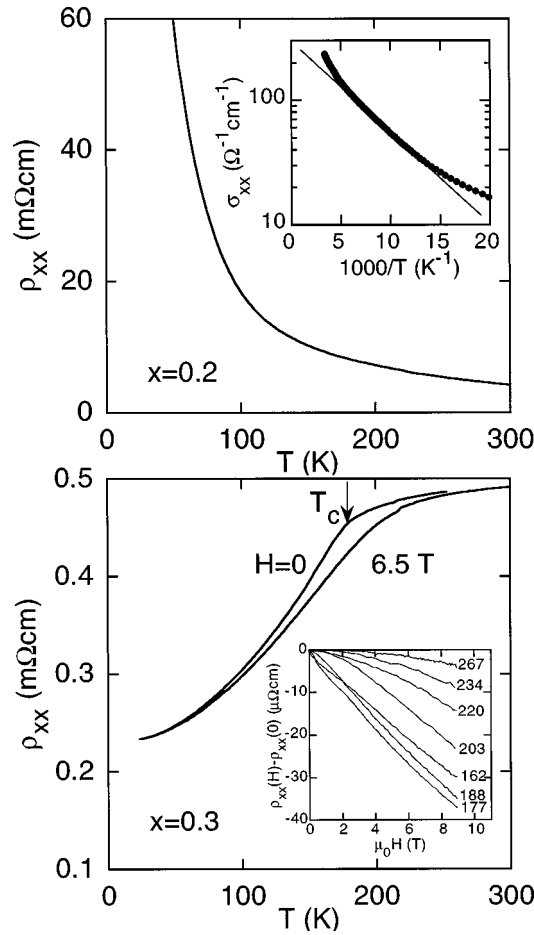


FIG. 1. The temperature dependence of the electrical resistivity ρ_{xx} in thin films: $x=0.2$ (top panel), $x=0.3$ (bottom panel). Inset of the top panel: the Arrhenius plot of the conductivity σ_{xx} . Inset of the bottom panel: the magnetoresistance in the $x=0.3$ sample.

size. Both the Hall resistance and magnetoresistance have similar behavior for $x=0.3$ and 0.5 . Therefore, in the following presentation we will concentrate mainly on the comparison of the samples with $x=0.2$ and 0.3 . For the Hall measurements, the electrical contacts are made by depositing four gold pads on the corners of the film, and the van der Pauw method is employed to measure both the Hall and longitudinal resistivities. The magnetic field is applied perpendicular to the surface of the films. The linear response of the system is verified by measuring the current-voltage characteristics in the current range of $0-30 \mu\text{A}$ at selected temperatures and magnetic fields. Magnetic measurements of the samples are carried out using a superconducting quantum inference device (SQUID) magnetometer. The total magnetic moments of the LCCO films-on-substrate, and those of a bare LaAlO_3 substrate with the same geometry, are measured. The diamagnetic background of the substrate is subtracted from the total signal, and the net magnetic moments of the films are divided by the sample volume to yield the magnetization.

Figure 1 (bottom panel) shows the temperature (T) dependence of the electrical resistivity ρ_{xx} of LCCO with $x=0.3$ in fields 0 and 6.5 T. A larger decrease in the resistivity on cooling through the Curie temperature T_c is observed, which may be attributed to the suppression of

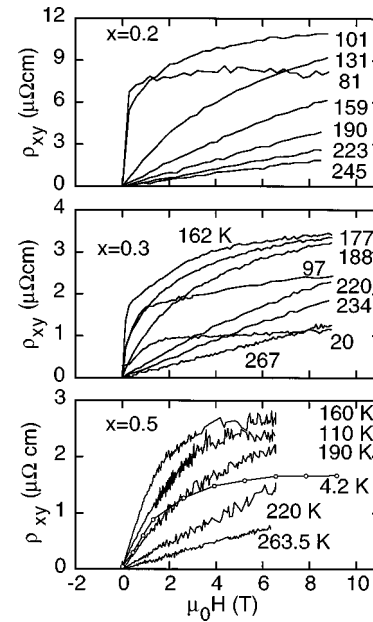


FIG. 2. The magnetic field dependences of the Hall resistivity ρ_{xy} of thin film samples with $x=0.2$ (top panel), $x=0.3$ (middle panel), and $x=0.5$ (bottom panel). The data are obtained in the zero-field-cooling mode.

disorder-spin scattering in the ferromagnetic phase. The negative magnetoresistance (Fig. 1, bottom panel, inset) can be understood within the double-exchange model;¹⁴ similar to the larger decrease of zero-field resistivity upon cooling through T_c , the application of an external magnetic field increases the magnetic order and hence reduces the electrical resistance. The negative magnetoresistance is the largest near T_c , consistent with maximum spin fluctuations near T_c .

Unlike in the sample with $x=0.3$, the resistivity in the film with $x=0.2$ increases upon cooling (Fig. 1, top panel). This behavior at low doping has been attributed⁹ to the trapping of Co^{4+} (and, consequently, holes) on divalent doping atoms. The electrical conduction occurs via the hopping motion of holes in the insulating matrix of low-spin, trivalent Co^{III} ions. Each hopping process consists of transferring the tetravalent configuration from one Co ion to another, accompanied by transforming of the neighboring Co^{III} ions into Co^{3+} ions.⁹ With increasing temperature, the ratio of Co^{3+} to Co^{III} ions in the matrix increases, facilitating the hopping process and increasing the conductivity. The activation energy determined from the Arrhenius plot at $75 \text{ K} < T < 200 \text{ K}$ (Fig. 1, inset of top panel) is about 0.016 eV , in agreement with Ref. 9.

The magnetic field (H) dependence of the Hall resistivity of thin film samples with $x=0.2, 0.3$, and 0.5 is presented in Fig. 2, showing ρ_{xy} linear in fields at sufficiently high temperatures. As temperature decreases towards T_c , nonlinearity in the field dependence becomes more pronounced. In the ferromagnetic state ($T < T_c$), the initial rapid rise in ρ_{xy} is followed by a much weaker field dependence with increasing field. In a separate experiment, the initial slope of the ρ_{xy} -vs- H curves in a $x=0.2$ sample, $\rho_{xy}/(\mu_0 H)$, has been measured in small fields up to $\pm 3 \text{ mT}$. The slope augments by two orders of magnitude upon cooling from $T=113 \text{ K}$ to $T=97 \text{ K}$, at which temperature it reaches a maximum value

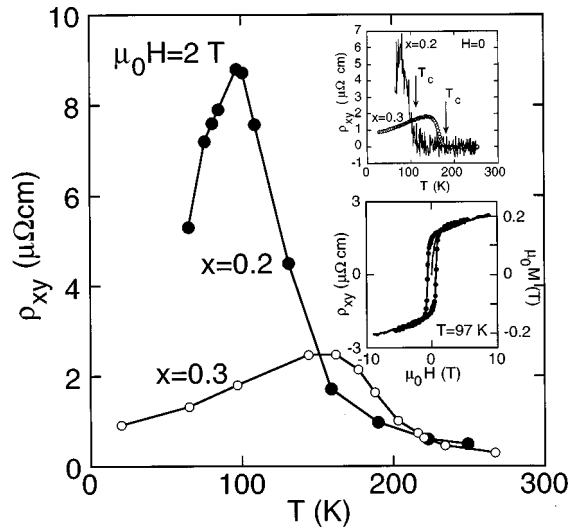


FIG. 3. The temperature dependence of the Hall resistivity in thin films with $x=0.2$ and $x=0.3$ in an applied field $\mu_0 H=2$ T. The upper inset shows the remanent Hall resistivity of the same sample in zero magnetic field, measured after field-cooling and subsequent reducing of the field to zero. The lower inset illustrates a hysteretic loop of $\rho_{xy}(H)$ (solid line) and $M(H)$ (circles) in the $x=0.3$ sample and at $T=97$ K $\ll T_c$.

$\rho_{xy}/(\mu_0 H) \approx 2 \times 10^{-6}$ m³/C = 200 $\mu\Omega$ cm/T. This large magnitude of $\rho_{xy}/(\mu_0 H)$ may be used for sensitive low-field magnetometers.

Typically in magnetic materials, the anomalous Hall effect is much more significant than the normal Hall contribution in the ferromagnetic state.⁷ We have verified that $R_s \gg R_0$,¹⁵ and that the Hall resistivity $\rho_{xy}(H)$ is strictly proportional to $M(H)$, both below and above T_c . The upper limit for the normal Hall effect is $R_0 < 0.2 \times 10^{-9}$ m³/C for $0.3 \leq x \leq 0.5$ and $R_0 < 0.4 \times 10^{-9}$ m³/C for $x=0.2$.

The ρ_{xy} -vs- H curves in Fig. 2 are taken after cooling the samples in a zero field. After each field sweep at a fixed temperature, ρ_{xy} demonstrates a hysteretic behavior which mimics that of the magnetization (Fig. 3, lower inset), and ρ_{xy} is not zero at $H=0$. This hysteretic behavior is consistent with the temperature dependence of the remanent Hall resistivity shown in the upper inset of Fig. 3: the samples are first cooled down in a field of several teslas, then the field is reduced to zero, and ρ_{xy} is measured upon warming. With increasing temperature, the Hall resistivity first increases, passing through a maximum, and then vanishes at $T_c \approx 110$ K and 180 K for $x=0.2$ and 0.3, respectively. In addition to the ρ_{xy} -vs- T measurements at $H=0$, the data are taken at a finite magnetic field $\mu_0 H=2$ T, as shown in the main panel of Fig. 3.

To obtain the temperature dependence of the anomalous Hall coefficient R_s , the magnetization of the LCCO thin films is measured using a SQUID magnetometer, as described previously. The results taken with $\mu_0 H=2$ T are shown in the inset of Fig. 4, and the corresponding R_s -vs- T data obtained by dividing $\rho_{xy}(H)$ by $\mu_0 M(H)$ are illustrated in the main panel of Fig. 4. We have also verified that $R_s(T)$ is independent of the applied field. $R_s(T)$ peaks near T_c for both $x=0.2$ and $x=0.3$. The decrease of $R_s(T)$ on cooling below T_c is typical for ferromagnetic metals. This fact, together with the fairly high carrier concentration $n=1/(R_0 e)$

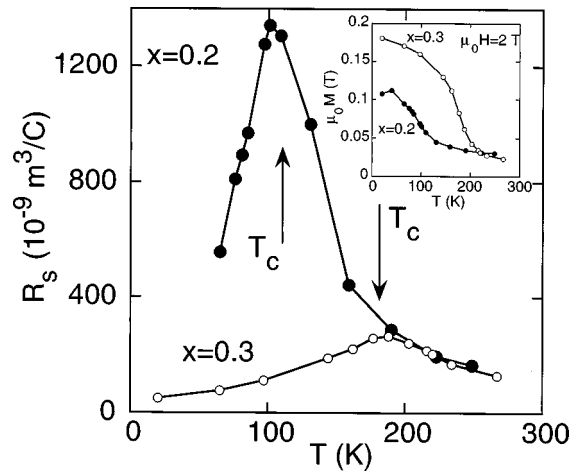


FIG. 4. The temperature dependences of the anomalous Hall coefficient R_s in the $\text{La}_{1-x}\text{Ca}_x\text{CoO}_3$ thin films with $x=0.2$ and 0.3. The inset shows the magnetization data of the same samples, taken under $\mu_0 H=2$ T using a SQUID magnetometer.

$> 1.5 \times 10^{28}$ m⁻³, allows the comparison with the theory for metals.

Within the model of Kondo¹² and Maranzana,¹³ the rise of R_s with temperature in the ferromagnetic state may be understood in terms of the spin-orbit interaction between the local spins and the carriers, which gives rise to the skew scattering of the latter and therefore the anomalous Hall effect.¹³ This model predicts monotonic increases of $R_s(T)$ on cooling below T_c , as well as of a maximum zero-field $\rho_{xy}(T)$ at $T \approx 0.8T_c$,^{12,13} qualitatively consistent with our experimental data. However, a large discrepancy exists in the magnitude of R_s between our experimental results and the theory.¹⁶ Another local electrons theory involves the side-jump mechanism (Ref. 17). It estimates the Hall resistivity in ferromagnets to be comparable to that due to skew scattering. Therefore, the side-jump term is also too small to account for the large values of the spontaneous Hall coefficient and Hall resistivity in LCCO.

An additional theory for the anomalous Hall effect in paramagnetic heavy-fermion compounds has been suggested by Coleman, Anderson, and Ramakrishnan¹⁸ and by Fert and Levy.¹⁹ The theory predicts the temperature dependence of the ratio ρ_{xy}/ρ_{xx} as that of the magnetic susceptibility. The comparison of two LCCO samples with $x=0.2$ and 0.3 (Figs. 1 and 2) clearly deviates from this theoretical prediction, because $\rho_{xx}(T)$ is very different between these samples, although ρ_{xy} has the same T dependence in the paramagnetic state (Fig. 3). Analogously, the itinerant electrons side-jump theory,⁸ which predicts a scaling relation, $\rho_{xy} \sim \rho_{xx}^2$, fails in the case of LCCO because the temperature- and doping-dependences of $\rho_{xy}(T, x)$ and $\rho_{xx}^2(T, x)$ are different. The lack of scaling of $\rho_{xy}(T)$ with either $\rho_{xx}(T)$ or $\rho_{xx}^2(T)$ may be due to a change in the carrier concentration with temperature. However, the suggestion of a constant hole density in a similar compound⁹ $\text{La}_{1-x}\text{Sr}_x\text{CoO}_3$ for 100 K $< T < 350$ K seems to rule out this scenario.

Although at present it is difficult to identify the underlying mechanism that determines the magnitude of R_s , we note that the anomalous Hall coefficients and Hall resistivities of all three LCCO films ($x=0.2, 0.3, 0.5$) are larger than

those of all other known ferromagnetic metals (see Ref. 20 for the R_s values of other materials), and that the only systems which show an R_s value comparable to ours are $\text{FeNi}-(\text{SiO}_2)_x$ granular films²¹ and $(\text{Fe-Ni})_3\text{O}_4$ compounds²² at low temperatures. The important difference between our results and that of Refs. 21 and 22 is the T dependence of R_s : In LCCO, R_s decreases upon cooling below T_c , whereas R_s increases with the decreasing temperature in Refs. 21 and 22. The large value of R_s and its temperature dependence of the latter systems have been attributed to the low electron density which decreases upon cooling.

Taking into account the metalliclike T dependence of R_s and relatively high carrier concentration $n > 1.5 \times 10^{28} \text{ m}^{-3}$, we suggest that in LCCO, it is the strong scattering rather than the low electron density that is responsible for the large spontaneous Hall effect. It is known that interfaces in magnetic heterostructures act as strong spin-orbit scatterers. We therefore speculate that the spin-orbit scattering at the interface between the low-spin and high-spin regions^{6,23} enhances the anomalous Hall effect. This conjecture is consistent with the enhancement of R_s near T_c where spin fluctuations are most significant, and with the fivefold increase in R_s with

decreasing doping level x from (0.3–0.5) to 0.2, the latter being near the ferromagnetic percolation threshold $x = 0.15$,^{9,11} where the decreasing size of magnetic clusters may result in an increasing spin-orbit scattering rate and therefore an enhanced R_s .

To summarize, we have observed an unprecedentedly large Hall effect in $\text{La}_{1-x}\text{Ca}_x\text{CoO}_3$ epitaxial films. The Hall effect is the largest at temperatures near T_c and for chemical compositions near the ferromagnetic percolation threshold, and the maximum magnitude is the largest among all known ferromagnetic metals. This phenomenon may be attributed to the unique spin configurations of the cobaltites, which give rise to an enhanced spin-orbit interaction at the interface between the low-spin and high-spin regions.

The research at Caltech was jointly supported by the National Aeronautics and Space Administration, Office of Space Science (NASA/OSS), Caltech President's Fund, and the Packard Foundation. Part of the research was performed at the Center for Space Microelectronics Technology, Jet Propulsion Laboratory, Caltech, under a contract with NASA/OSS.

- ¹R. von Hemlolt *et al.*, Phys. Rev. Lett. **71**, 2331 (1993); H. L. Ju *et al.*, Appl. Phys. Lett. **65**, 2108 (1994); H. Y. Hwang *et al.*, Phys. Rev. Lett. **75**, 914 (1995).
- ²M. N. Baibich *et al.*, Phys. Rev. Lett. **61**, 2472 (1988); S. S. Parkin, N. More, and K. P. Roche, *ibid.* **64**, 2304 (1990); A. E. Berkowitz *et al.*, *ibid.* **68**, 3745 (1992).
- ³M. Jaime *et al.*, Phys. Rev. Lett. **78**, 951 (1997).
- ⁴L. E. Núñez-Regueiro, D. Gupta, and A. M. Kadin, J. Appl. Phys. **79**, 5179 (1996).
- ⁵F. Tsui *et al.*, Phys. Rev. Lett. **72**, 740 (1994).
- ⁶J.-Q. Wang and G. Xiao, Phys. Rev. B **51**, 5863 (1995).
- ⁷C. M. Hurd, *The Hall Effect in Metals and Alloys* (Plenum Press, New York, 1972).
- ⁸L. Berger, Phys. Rev. B **2**, 4559 (1970); A. K. Majumdar and L. Berger, Phys. Rev. B **7**, 4203 (1973); for review, see A. Fert and D. K. Lottis, in *Concise Encyclopedia of Magnetic and Superconducting Materials* (Pergamon Press, New York, 1992), p. 287.
- ⁹M. A. Señaris-Rodríguez and J. B. Goodenough, J. Solid State Chem. **118**, 323 (1995).
- ¹⁰M. Itoh *et al.*, J. Phys. Soc. Jpn. **63**, 1486 (1994).
- ¹¹H. Taguchi, M. Shimada, and M. Koizumi, J. Solid State Chem. **41**, 329 (1982).
- ¹²J. Kondo, Prog. Theor. Phys. **27**, 772 (1962).
- ¹³F. E. Maranzana, Phys. Rev. **160**, 421 (1967).
- ¹⁴G. H. Jonker and J. van Santen, Physica (Amsterdam) **16**, 337 (1950); C. Zener, Phys. Rev. **82**, 403 (1960); P.-G. de Gennes, *ibid.* **118**, 141 (1960); A. J. Millis, P. B. Littlewood, and B. I. Shraiman, Phys. Rev. Lett. **74**, 5144 (1995).
- ¹⁵A. V. Samoilov, N.-C. Yeh, and R. P. Vasquez, in *Epitaxial Oxide Thin Films—III*, edited by C. Foster, J. S. Speck, D. Schlom, C.-B. Eom, and M. E. Hawley, MRS Symposia Proceedings No. 474 (Materials Research Society, Pittsburgh, 1997).
- ¹⁶According to Ref. 13, $R_s = \rho_{xy}/(\mu_0 M) = [3 \sin(k_F a)/\text{Ne}] [J^2/E_F E_0]/[g M_3(T)/\sigma(T)]$. Here, k_F is the Fermi vector, a is the lattice constant, $N = a^{-3}$ is the concentration of magnetic (cobalt) ions, J is the constant of the exchange coupling between the localized moments and the spins of conduction electrons, E_F is the Fermi energy, $E_0 = \hbar^2/(ma^2)$, m is the electron mass, g is the g factor, $M_3(T)$ is the (dimensionless) three-point correlation function computed in Ref. 13, and $\sigma(T) = M_s(T)/M_s(0)$ is the reduced magnetization, and $g M_3(T)/\sigma(T)$ increases from 0 to ~ 0.25 with the increasing temperature from 0 to T_c . $J^2/E_F N$ may be estimated from the resistivity due to spin scattering: $\rho_m \sim mJ^2/e^2 \hbar E_F N$ (Ref. 17). With $\rho_m \sim 0.2 \text{ m}\Omega \text{ cm}$ for $x = 0.3\text{--}0.5$, $g = 2$, $\sin(k_F a) = 1$, we obtain a theoretical estimate $R_s \approx 3 \times 10^{-10} \text{ m}^3/\text{C}$.
- ¹⁷A. Fert, J. Phys. (France) **35**, L107 (1974).
- ¹⁸P. Coleman, P. W. Anderson, and T. V. Ramakrishnan, Phys. Rev. Lett. **55**, 414 (1985).
- ¹⁹A. Fert and P. M. Levy, Phys. Rev. B **36**, 1907 (1987).
- ²⁰The maximum R_s (in $10^{-9} \text{ m}^3/\text{C}$) values of various magnetically ordered metals: Gd single crystal: 40 (Ref. 24); single crystal and polycrystal Fe: ≈ 0.5 (Ref. 7); polycrystal Ni: ≈ 0.6 (Ref. 7); multilayer Co/Cu: 0.4 (Ref. 5); single crystal CoS_2 : 120 (Ref. 25); epitaxial films $\text{La}_{2/3}\text{Ca}_{1/3}\text{MnO}_3$: < 40 (Ref. 4).
- ²¹A. B. Pakhomov, X. Yan, and Y. J. Xu, J. Appl. Phys. **79**, 6140 (1996); X. N. Jing *et al.*, Phys. Rev. B **53**, 14 032 (1996). R_s is $1650 \times 10^{-9} \text{ m}^3/\text{C}$ and n is $(3\text{--}6) \times 10^{26} \text{ m}^{-3}$ in $\text{FeNi}-(\text{SiO}_2)_x$ at $T = 5 \text{ K}$.
- ²²J. M. Lavine, Phys. Rev. **123**, 1273 (1961). R_s is $260 \times 10^{-9} \text{ m}^3/\text{C}$ and $1300 \times 10^{-9} \text{ m}^3/\text{C}$, $n = 4 \times 10^{27} \text{ m}^{-3}$ and $3 \times 10^{26} \text{ m}^{-3}$ in Fe_3O_4 and $\text{Ni}_{0.25}\text{Fe}_{2.25}\text{O}_4$, respectively, at $T = 300 \text{ K}$. R_s grows by a factor ≈ 2 with temperature decrease down to $\approx 150 \text{ K}$.
- ²³G. Bergman and C. Horriar-Esser, Phys. Rev. B **31**, 1161 (1985); P. E. Lindelof and S. Wang, *ibid.* **33**, 1478 (1986).
- ²⁴R. S. Lee and S. Legvold, Phys. Rev. **162**, 431 (1967).
- ²⁵K. Adachi and K. Ohkohchi, J. Phys. Soc. Jpn. **49**, 154 (1980).